AGU PUBLICATIONS

JGR

Journal of Geophysical Research: Atmospheres

RESEARCH ARTICLE
10.1002/2015JD024648

Key Points:
- The recently observed warming over the Baltic Sea region has most likely an anthropogenic origin
- The effect of an anthropogenic signal is detectable in surface solar radiation, which is not GHG

Supporting Information:
- Supporting Information S1

Correspondence to:
A. Barkhordarian,
barkhora@g.ucla.edu

Citation:
Barkhordarian, A., H. von Storch, E. Zorita, and J. J. Gómez-Navarro (2016), An attempt to deconstruct recent climate change in the Baltic Sea basin, *J. Geophys. Res. Atmos.*, *121*, 13,207–13,217, doi:10.1002/2015JD024648.

Received 13 DEC 2015
Accepted 24 OCT 2016
Accepted article online 27 OCT 2016
Published online 17 NOV 2016

An attempt to deconstruct recent climate change in the Baltic Sea basin

A. Barkhordarian[1,2,3], H. von Storch[1], E. Zorita[1], and J. J. Gómez-Navarro[4,5]

[1]Institute of Coastal Research, Helmholtz-Zentrum Geesthacht, Geesthacht, Germany, [2]Now at Department of Atmospheric and Oceanic Sciences, University of California Los Angeles, California, USA, [3]Also at Jet Propulsion Laboratory, California Institute of Technology, Pasadena, California, USA, [4]Climate and Environmental Physics, Physics Institute and Oeschger Centre for Climate Change Research, University of Bern, Bern, Switzerland, [5]Now at Department of Physics, University of Murcia, Spain

Abstract We investigate whether the recently observed temperature and precipitation trends over the Baltic Sea Basin are consistent with state-of-the-art regional climate model projections. To address this question we use several data sources: (1) multidecadal trends derived from various observational data sets, (2) estimates of natural variability provided by a 2000 year paleoclimatic model simulation, and (3) response to greenhouse gas forcing derived from regional climate simulations driven by the A1B and RCP4.5 scenarios (from ENSEMBLES and CORDEX projects). Results indicate that, over the past decades, the climate in the Baltic Sea Basin has undergone a change that is beyond the estimated range of natural variability. We test the hypothesis that this change may be understood as a manifestation of global warming due to increasing concentrations of greenhouse gases (GHGs). We find that changes in near-surface temperature support our hypothesis that the effect of GHG is needed to simulate the observed changes. The pattern correlation and regression results clearly illustrate the concerted emergence of an anthropogenic signal consistent with the GHG signal in summer and autumn in the 21st century. However, none of the 19 regional climate simulations used in this study reproduce the observed warming. The observed trends in precipitation and surface solar radiation are also partially inconsistent with the expected changes due to GHG forcing. We conclude that, besides the regional response to GHG forcing, other human-made drivers have had an imprint. Regional emission of industrial aerosols has been strongly reduced in this region, and we suggest that this reduction may be the missing driver.

1. Introduction

There is a large body of literature on climate change at the global scale [*Intergovernmental Panel on Climate Change*, 2013]. However, local feedbacks and forcings can lead to very different climate change responses in different parts of the world [*Stott et al*., 2010]. Successful adaptation to climate change requires an understanding of such regional differences. However, there are still important uncertainties affecting the range of predicted climate change at regional scales due to missing or not properly reproduced regional feedbacks and external forcings in climate models. One example is land use changes, such as urbanization and the associated pollution. Another source of uncertainty is the heterogeneous spatial impact of anthropogenic and natural aerosols, such as those produced by dust storms, fires, and explosive volcanic eruptions. In spite of these limitations, climate models are currently the best available tool to produce climate change projections at regional scale, and these climate projections encapsulate our best assumptions of future emission scenarios.

A comprehensive summary of climate scenarios for the Baltic Sea Basin has been published in the BALTEX second assessment of the climate change for the Baltic Sea Basin [*BALTEX Assessment of Climate Change* (*BACC*) 2015]. As stated in *BACC* [2015], the effect of external forcing on European temperature has been investigated by *Hegerl et al*. [2011]. They use reconstructed temperature back to A.D. 1500 and detected external influences in all seasons, with the response to external forcing explaining about 30% of the interdecadal temperature variance. As summarized in *BACC* [2015], the observed warming over the Baltic Sea Basin has also been found to be consistent with anthropogenic signals derived from simulations with a coupled regional atmosphere-ocean model by *Bhend and von Storch* [2009], whereas *van Oldenborgh et al*. [2009] found, using global climate models (GCMs), significant differences between observed and simulated warming in spring in this region (MAM). They identified the misrepresentation in atmospheric circulation and snow cover changes as the main reason for the underestimation of warming in spring by

Table 1. List of the Regional Climate Models (RCMs) and of Their Driving General Circulation Models (GCMs)

WCRP CORDEX (RCP4.5)			ENSEMBLES (A1B)		
Institute	RCM	Driving GCM	Institute	RCM	Driving GCM
SMHI	RCA4	CCCma-CanESM2	C4I	RCA**3**	HadCM3Q16
SMHI	RCA4	CNRM-CERFACS	CNRM	ALADIN	ARPEGE_RM5.1
SMHI	RCA4	ICHEC-EARTH	DMI	HIRHAM5	ECHAM5
SMHI	RCA4	IPSL-CM5A-MR	DMI	HIRHAM5	ARPEGE
SMHI	RCA4	MIROC-MIROC5	ETHZ	CLM	HadCM3Q0
SMHI	RCA4	MOHC-HadGEM2	KNMI	RACMO	ECHAM5-r2
SMHI	RCA4	MPI-ESM-LR	KNMI	RACMO	MIROC3
SMHI	RCA4	NCC-NorESM1-M	HC	HadRM3	HadCM3Q0
SMHI	RCA4	GFDL-ESM2M	MPI-M	REMO	ECHAM5
			SMHI	RCA**3**	ECHAM5-r3

global climate models. A study by *Flanner et al*. [2009] suggested that the underestimation of springtime warming at midlatitudes is due to the lack of carbonaceous aerosols in climate model simulations.

In this study, we employ regional climate models to assess the role of greenhouse gas (GHG) forcing on recently observed trends over the Baltic Sea Basin and to examine to what extent the present climate change "is on the way" toward conditions described by state-of-the-art regional climate change scenarios at the end of this century. The approach used here has been previously applied over the Mediterranean region [*Barkhordarian et al*., 2012a, 2012b; *Barkhordarian*, 2012; *Barkhordarian et al*., 2013]. In those studies, it was determined that the recently observed warming and the increase in surface specific humidity over the Mediterranean region very likely have an anthropogenic origin [*Barkhordarian et al*., 2012a, 2012b]. In terms of precipitation, whereas the anthropogenic signal is detectable in the observations, observed precipitation changes are several times larger than the simulated response to anthropogenic forcing [*Barkhordarian et al*., 2013].

Here we investigate for the first time the consistency of observed (temperature, precipitation, and surface solar radiation) trends over the Baltic Sea Basin and climate change projections with both Intergovernmental Panel on Climate Change (IPCC) Special Report on Emissions Scenarios (SRES) and Representative Concentration Pathways (RCPs). The main task of climate change projections is to help policymakers and planners in coping with the perspectives and consequences of expected future climate change. Therefore, investigating the consistency of ongoing changes with climate change projections is an issue of significant societal importance. By linking past changes to expected future changes, this study helps to provide an illustrative example of what a potential future climate influenced by enhanced greenhouse gas concentration might look like.

2. Observations and Model Data

Our studied domain encompasses the Baltic Sea Basin, defined here as the region from 50°N to 70°N and 3°E to 38°E, which lies between maritime temperate and continental subarctic climate zones. The observed temperature and precipitation data set used here consists of the latest version of the Climate Research Unit's (CRU) gridded high-resolution (0.5° by 0.5°) data set CRU TS 3.22, available from 1901 to 2013 [*Harris et al*., 2014]. The station records of the CRU TS 3.22 data sets are quality controlled and homogenized using the automated method proposed in *Easterling and Peterson* [1995]. We also use version 11.0 of E-OBS daily gridded observational data set for precipitation and temperature on a 0.5° (latitude) by 0.5° (longitude) grid available from 1950 to 2014 [*Haylock et al*., 2008]. For surface solar radiation a 30 year long (1984–2013) continuous and validated climate data record (CDR) based on the Meteosat First Generation satellites is used [*Posselt et al*., 2011].

For the climate change projections, we consider 10 regional climate simulations covering the period 1950–2100 from the EU-FP6 ENSEMBLES project [*Kjellström et al*., 2013] based on the SRES A1B emission scenario [*Nakicenovic et al*., 2000]. Additionally, nine regional climate simulations from the World Climate Research Program, COordinated Regional climate Downscaling Experiment (WCRP EURO-CORDEX) [*Jones et al*., 2011; *Jacob et al*., 2014] are used, which include projections driven by future GHG atmospheric concentrations following the Representative Concentration Pathway 4.5 (RCP 4.5) [*Meinshausen et al*., 2011]. A list of the regional climate models, driven by different general circulation models (GCMs), is given in Table 1. Previously to the analysis, the model data were interpolated onto a latitude-longitude grid with a resolution of 0.5° using conservative remapping [*Jones*, 1999].

We follow the same approach presented in *Barkhordarian et al*. [2012a, 2012b], *Barkhordarian* [2012], and *Barkhordarian et al*. [2013]. In the first step we assess how likely the observed changes are, assuming they are manifestations of natural variability. For this purpose, the observed trends are compared with the distribution of simulated natural (internal + external) variability derived from a 2000 year high-resolution regional climate Paleosimulation [*Gómez-Navarro et al*., 2013, 2015a]. High-resolution regional climate models render our analysis more coherent because they have more realistic land sea mask in the Baltic Sea region that increases the spatial variability compared to GCMs. In addition, Paleosimulations have comparable resolution as in the regional climate projections (CORDEX, ENSEMBLES).

The 2000 year simulation encompasses almost entirely the European region with a spatial resolution of 45 km and employs the same configuration as that thoroughly described by *Gómez-Navarro et al*. [2013, 2015b]. The simulation was carried out with a climate version of the MM5 (Mesoscale Meteorological Model, Version 5) model, and it is driven at the boundaries by the global model ECHO-G. The atmospheric component of ECHO-G is ECHAM4 [*Roeckner et al*., 1996], and the oceanic component is HOPE-G [*Legutke and Maier-Reimer*, 1999]. Both MM5 and ECHO-G simulations are consistently driven by reconstructions of greenhouse gas concentrations, variations in the total solar irradiance at the top of the atmosphere, and changes in the Earth's orbital parameters. However, it does not consider volcanic forcing due to the lack of reliable reconstructions of this factor for the first millennium. However, as shown in Figures S1 and S2 (supporting information), the inclusion of volcanoes does not have noticeable impact in the width of the distribution, indicating that the lack of volcanic activity is not a limitation of the data set we are using in this study, which, on the other hand, has the advantage to begin longer and thus have a more statistically representative record. In order to exclude the effect of anthropogenic forcing, only the period before the industrialization (before 1800 A.D.) is used. Thus, the preindustrial variability, derived from the 1800 year Paleosimulation, includes natural (internal + external) variability and explicitly excludes anthropogenic factors.

The ability of this simulation to mimic the variability of the climate system is a key aspect for the suitable application of the methodology used in this study. Thus, the skill of this model setup has been previously addressed by comparing the seasonal variability of the simulated temperature and precipitation with the CRU data set, i.e., Figures 3, 4, 6, and 7 in *Gómez-Navarro et al*. [2013] and Figures 8 and 9 in *Gómez-Navarro et al*. [2015b]. Those previous studies pointed out how the model is able to reproduce the main temperature and precipitation patterns over Europe, as well as their main modes of variability during the last centuries previous to the large impact of anthropogenic activities [*Gómez-Navarro et al*., 2015b, Figures 8 and 9]. We outline here the largest systematic biases reported for this simulation. They appear in winter [*Gómez-Navarro et al*., 2013, Figure 6], when the model underestimates interseasonal variability of temperature at decadal timescales. Still, this error does not impact the conclusions drawn by this study (as discussed in section 4.3). Precipitation variability at decadal timescales within the domain exhibits positive and negative biases with respect to the observations, and thus, there are no systematic biases in precipitation variability that might potentially bias our conclusions [*Gómez-Navarro et al*., 2013, Figure 7].

3. Methodology

In the first step we will assess whether the observed changes over the Baltic Sea Basin are compatible with an undisturbed stationary climate. This is achieved by testing whether the observed changes are significantly different from changes due to natural variability alone—detection. This "detection" step can be phrased as a statistical test with the null hypothesis H_0: zero trends. To test the null hypothesis, annual and seasonal observed mean trends are compared with a distribution of trends generated by "preindustrial variability" derived by the 1800 year high-resolution regional climate Paleosimulation (section 2). For the comparison of the observed and simulated trends, the temperature (precipitation, solar radiation) series for the Baltic Sea Basin is obtained from the 1800 year Paleosimulation. Then the series is split into 60 nonoverlapping 30 year segments, and the trends for each 30 year period are calculated. We use these 60 sampled trends as an estimation of the amplitude of preindustrial variability corresponding to periods of 30 year trends. If the observed trend lies above the 95th percentiles of this distribution of trends, the null hypothesis is rejected indicating that there is less than a 5% chance (one-tailed test) that natural variability rather than an anthropogenic driver is responsible for the observed changes.

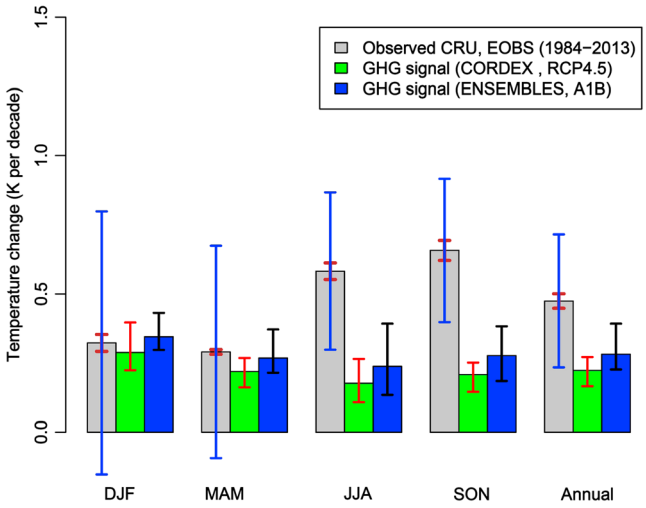

Figure 1. Observed area-averaged changes of near-surface temperature over the period 1984–2013 (gray bars) in comparison with GHG signal estimated from nine CORDEX simulations based on RCP4.5 (green bars), 10 ENSEMBLES projections based on SRES A1B (blue bars). The brown whiskers denote the spread of trends of the two observational data sets (CRU, EOBS). The blue whiskers indicate the 95th percentile uncertainty range of observed trends, derived from 1800 year paleoclimatic model simulations. The red and black whiskers show the spread of trends of nine RCP4.5 and 10 A1B climate change projections. Units are K/decade.

Once it is found that anthropogenic forcing is very likely necessary for explaining recent trends, we will assess in the next step whether these results are consistent with GHG signals derived from the former (A1B) and more recent (RCP 4.5) generation of regional climate scenarios. The anthropogenic (GHG) climate change signal is defined here as the simulated difference between the last three decades of the 21st century (2071–2100) and the reference climatology (1961–1990). The resulting signal is expressed in terms of units change per decade [*Bhend and von Storch*, 2008; *Barkhordarian et al*., 2013]. The comparison between observed and GHG signal patterns are carried out using correlation and regression indices (for more details, see *Barkhordarian et al*. [2012b]).

4. Results (Temperature)

4.1. Detection of Anthropogenic Effect

The comparison of the observed spatially averaged change of the seasonal near-surface temperature over the period from 1984 to 2013 and the multimodel ensemble mean response to GHG forcing (2071–2100 minus 1961–1990, signal scaled to change per decade) derived from the 10 A1B (ENSEMBLES) and the nine RCP4.5 (CORDEX) scenarios is shown in Figure 1. Over the Baltic Sea Basin, observed temperature (T) trends derived from both CRU and E-OBS data set exhibit warming in all seasons, with maximum warming in autumn and minimum in spring (Figure 1). Warming is observed and also projected by regional climate models based on both A1B and RCP4.5 scenarios for all seasons as response to GHG forcing (Figure 1). Here we assess whether the observed trends are within the range of trends consistent with only "preindustrial variability." The observed warming is likely not due to natural variability alone in those cases where the 95th percentile confidence interval (blue whiskers in Figure 1, one-tailed test) derived from Paleosimulations (60 nonoverlapping 30 year segments) excludes zero.

As shown in Figure 1, the 95th percentile confidence interval (blue whiskers) derived from Paleosimulations excludes zero in summer (JJA, June-July-August) and autumn (SON, September-October-November). This indicates that no single sample of the sixty 30 year segments yield a positive trend of temperature as strong as that observed during the period 1984–2013. Thus, we conclude that the null hypothesis of a trend produced by natural forcing without any anthropogenic effect can be ruled out (with a probability of error below 5%). Therefore, anthropogenic forcing is detectable in the observed temperature trends in summer and autumn. However, in winter (DJF, December-January-February) and spring (MAM, March-April-May), the observed positive trends lie within the range of trends solely due to natural variability. Having established that human-induced changes are detectable in the observed record, we will proceed to a "consistency" step by checking whether the detected changes are consistent with what climate models describe as the expected response to GHG forcing.

4.2. Consistency of Observed and GHG Signal

This section compares the observed temperature trends with those downscaled under the climate change scenarios A1B and RCP4.5. The anthropogenic (GHG) climate change signal is defined here as the average difference between the last decades of the 21st century (2071–2100) and the reference climatology (1961–1990), expressed as degrees per decade. The comparison between the spatial patterns of observed

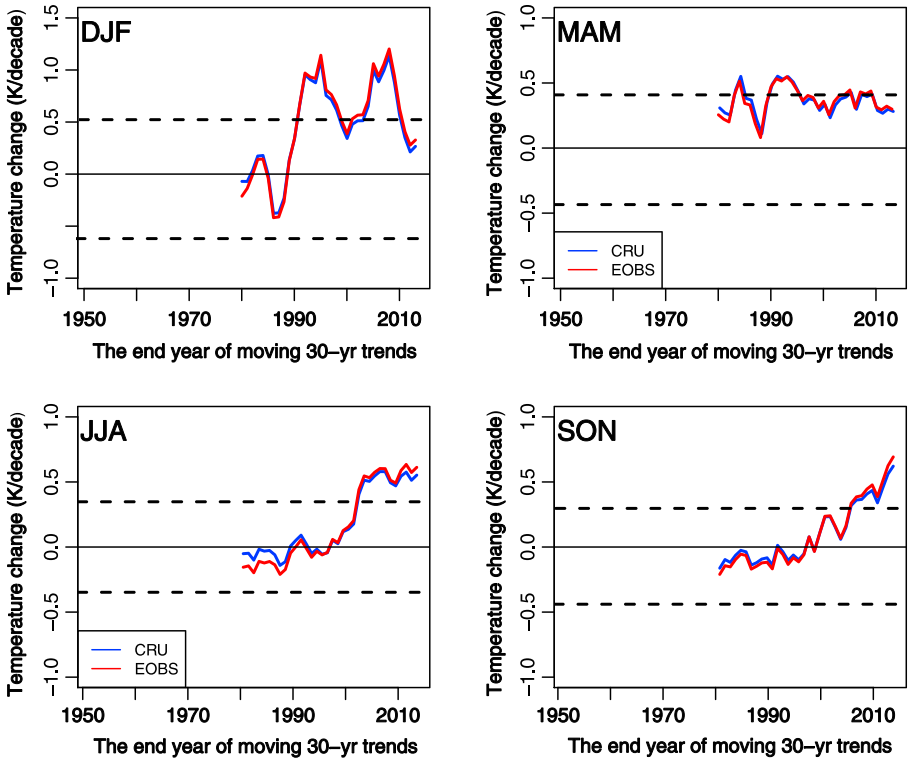

Figure 2. Seasonal 30 year gliding trends based on CRU (blue curves) and EOBS (red curves) from 1950 to 2013. The vertical axes denote the area-mean temperature change over the Baltic region. The horizontal axes show the end year of gliding 30 year segments. The dotted horizontal lines indicate the 95th percentile uncertainty range of observed trends (natural variability), derived from 1800 yearlong paleosimulations. The observed trends are very likely not due to natural variability alone in cases if its magnitude is larger than the dotted lines.

seasonal warming trends and of the simulated GHG signal is carried out using correlation coefficients (for more details, see *Barkhordarian et al.* [2012a]). In summer (JJA) the correlation between the observed pattern of temperature trend with the nine GHG signal patterns (nine simulations from CORDEX) are in the range of [0.93, 0.96]. These correlations are larger than the 95th percentile distribution of correlation coefficients obtained between the GHG signal pattern and the 60 trend patterns (the spatial patterns of seasonal changes in 30 year segments) derived from Paleosimulations in the preindustrial period. The highest positive correlation is found in autumn, with the nine correlation coefficients being in the range of [0.95, 0.97]. Also, in autumn the correlation between the GHG signal pattern and the 60 trend patterns derived from preindustrial variability is never as high as with the observed trend patterns. Indeed, such correspondence can hardly be expected to occur (with $<$5% risk of error) if the effect of GHG signal were not present in the observed warming in JJA and SON over the Baltic Sea Basin. However, in DJF and MAM the correlation coefficients are lower and not statistically significant (Figure 3).

4.3. Dependence on the Period to Calculate Trends

We further analyze how dependent our results are on the exact time period under analysis. Figure 2 shows, for each season, the observed temperature trends calculated over gliding 30 year periods based on CRU and E-OBS over the period 1950–2013. The two observation data sets show good agreement. Note that the observed trends are considered not due to natural variability only in those cases in which the trend is beyond the 95th percentile distribution of preindustrial variability (as denoted by the horizontal dashed lines in Figure 2 and estimated from the 1800 year paleosimulation, two-tailed test).

In the late twentieth century and the beginning of 21st century, the maximum warming is observed in winter (Figure 2), and trends are significantly different from what is expected from natural variability alone. The strongest 30 year trend of about 1.2°C/decade is observed during 1968–1997 and 1980–2009 period in

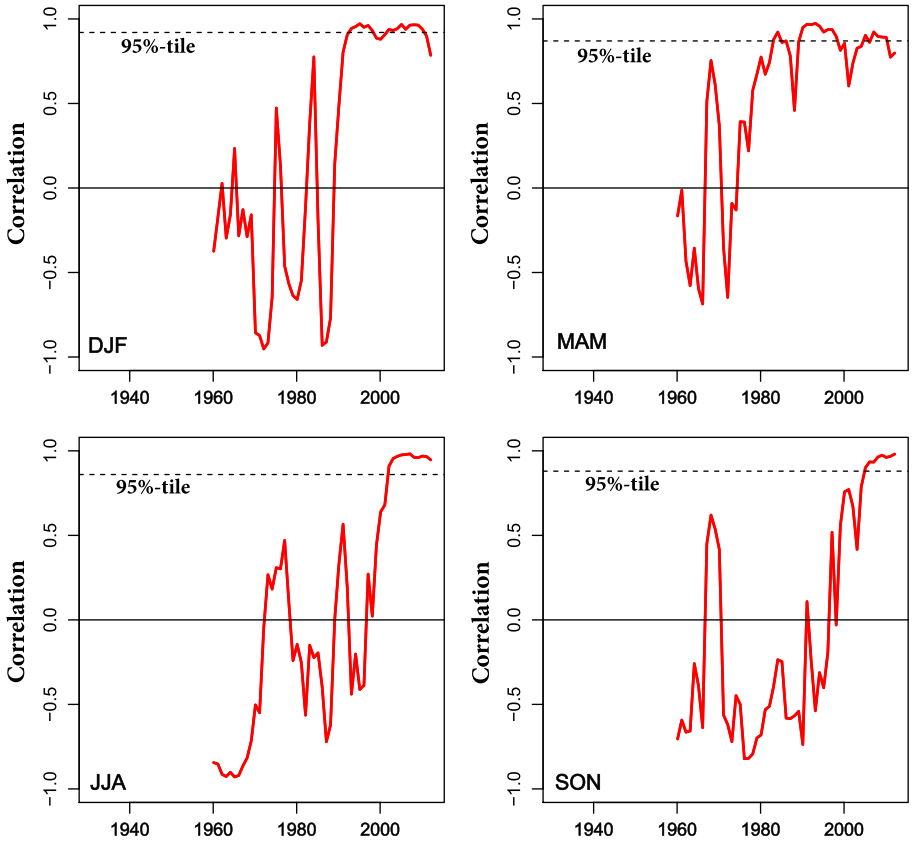

Figure 3. Seasonal correlation coefficients between the mean pattern of the multimodel temperature response to GHG forcing and the gliding 30 year trend patterns, based on CRU over 1950–2013. The horizontal axes show the end year of moving 30 year segments. The dashed horizontal lines indicate the 95th percentile distribution of correlation coefficients between the 60 naturally forced trend patterns, derived from the 1800 year paleosimulations, and the ensemble mean GHG response pattern.

winter, which can hardly be explained as a result of natural variability alone (Figure 2). However, the unusually cold regional weather in 2011 and early January 2012 almost all over Europe led to a change also in long-term 30 year trends. For 1984–2013 both data sets show that long-term warming, in contrast to the earlier periods, has its maximum in summer/autumn and minimum in winter/spring. An incursion of cold polar air coming from northern Russia area brought extremely low temperatures in winter over large parts of Europe and is responsible for the smaller trend in recent winters, which is not significant any more (Figure 1). Another potential driver of the recent severe winter weather could be the AMO (Atlantic Multidecadal oscillation), that is currently in positive polarity (warm Atlantic SST), resulting in negative NAO—and blocking episodes in winter [*Peings and Magnusdottir*, 2014].

In summer (JJA) and autumn (SON), both data sets show positive 30 year trends starting in the late twentieth century (Figure 2). The warming rate increases with time and first exceeds the limits of trends due to natural variability alone for the 30 year segment ending in 2003 for summer, and in 2006 in autumn, remaining significant for later 30 year segments. Evidence for the presence of an anthropogenic driving factor is clearly detectable in the late twentieth century and the beginning of 21st century in summer and autumn at the 5% significant level. However, the observed trends in spring (MAM) are hardly distinguishable from trends due to natural variability alone (Figure 2).

In the following, we assess to what extent the observed moving 30 year temperature trends over the 1950–2013 period are consistent with GHG climate change as defined by the ensemble mean of Regional Climate Models (RCMs) simulations. The comparison of observed temperature trend patterns with the spatial GHG signal is carried out using correlation and regression indices. Figure 3 displays the seasonal correlation coefficients between the observed patterns of 30 year temperature trend and the

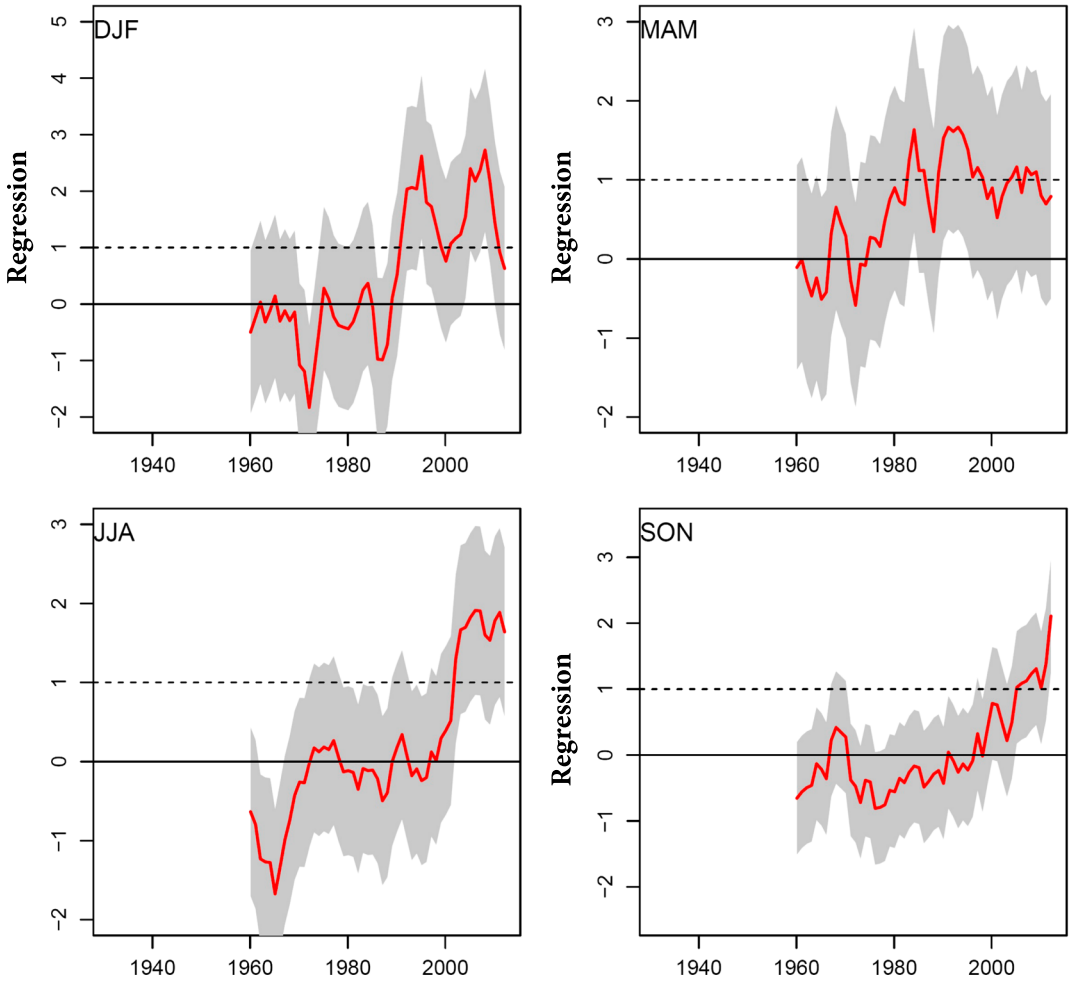

Figure 4. Seasonal regression indices of gliding 30 year temperature trend patterns based on CRU over 1950–2013 onto the ensemble mean GHG response pattern. The horizontal axes show the end year of moving 30 year trends. The gray-shaded area indicates the 95th percentile distribution of regression indices, derived from fits of 60 naturally forced 30 year trend pattern, obtained from the 1800 year paleosimulations, onto the ensemble mean GHG response pattern. Detection of a nonnatural signal can be claimed in those cases where the gray-shaded area excludes "0" and consistency with GHG signal is claimed in cases where the gray-shaded area does not include "0" but includes "1."

GHG signal derived from the multimodel mean response to GHG forcing (ensemble mean of nine simulations from the CORDEX project). The dashed horizontal lines indicate the 95th percentile distribution of correlation coefficients between the 60 naturally forced 30 year trend patterns, derived from paleosimulations, and the multimodel mean response pattern to GHG forcing. As shown in Figure 3 in DJF and MAM the correlation indices are, with a few exceptions, never significantly different from zero. However, in JJA and SON the high positive correlation coefficients exceed the limit of correlations due to natural variability (dashed horizontal lines in Figure 3) for 30 year trends ending in 2002 and for subsequent 30 year segments.

We further use regression indices which, unlike the correlation statistics, measure the relative magnitude of the observed and model-projected trend patterns. Figure 4 shows, for each season separately, the regression indices of observed moving 30 year trend pattern, over the period 1950–2013, onto the multimodel mean GHG signal pattern (ensemble mean of nine models from CORDEX project). The gray-shaded area indicates the 95th percentile uncertainty range of those regression indices. This range is derived from fits of the regression model to 60 naturally forced 30 year trend patterns, obtained from the paleosimulation, onto the GHG signal patterns. Detection of a nonnatural signal can be claimed in those cases where the gray-shaded area excludes "0," and consistency with GHG signal is claimed in cases where the gray-shaded area in Figure 4

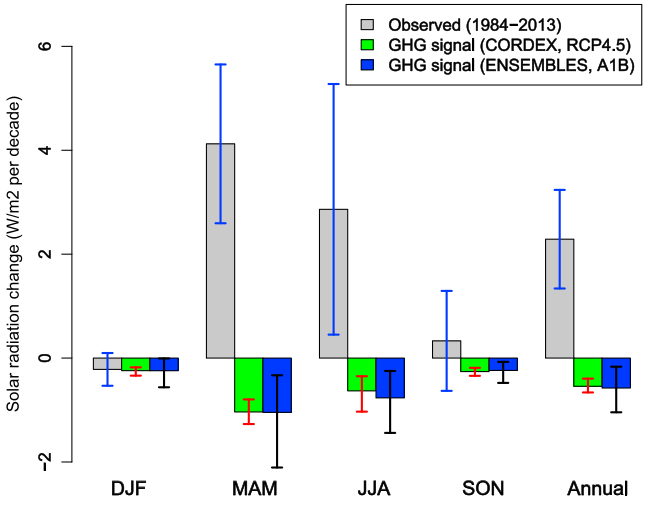

Figure 5. Seasonal area-mean changes of observed Surface Solar Radiation (SSR, in W/m^2/decade) according to CDR satellite data over the period 1984–2013 (gray bars) compared to the GHG response estimated from nine CORDEX simulations driven by RCP4.5 (green bars), 10 ENSEMBLES projections based on SRES A1B (blue bars). The blue whiskers indicate the 95th percentile uncertainty range of the observed trend, derived from the 1800 yearlong paleosimulations. The red and black whiskers show the spread of trends of nine RCP4.5 and 10 A1B climate change projections.

does not include "0" but includes "1." In JJA and SON, the gray-shaded area does not include the zero line (Figure 4) but includes a regression coefficient of 1 for 30 year trends ending in 2002 and later, indicating the emergence of a detectable anthropogenic (GHG) influence in the 21st century in the warm seasons over the Baltic Sea Basin. The pattern correlation (Figure 3) and pattern regression (Figure 4) results clearly illustrate the concerted emergence of an anthropogenic signal consistent with the GHG signal in the 21st century in JJA and SON. In section 5 we assess the observed and projected surface solar radiation (SSR) changes over the Baltic Sea Basin.

5. Surface Solar Radiation (Direct Effect of Aerosols)

The sum of the direct and diffuse radiation incident on the surface is denoted as Surface Solar Radiation (SSR). To our knowledge, no study exists that assesses the consistency of observed SSR trends with climate change projections over the Baltic Sea Basin. Basically, changes in SSR can either be caused by extraterrestrial changes in the amount of solar radiation at the top of the atmosphere or by internal changes within the climate system. Extraterrestrial changes depend on the Earth's orbital parameters, which vary substantially on geological timescale of longer than 10,000 years and can thus be neglected in the interpretation of the observed changes on the decadal timescale considered here [*Wild et al.*, 2005]. Although solar activity does vary at all timescales, at decadal timescales regional SSR changes are mostly a result of changes in the atmospheric transparency due to cloud changes and/or changes in the anthropogenic aerosols. These can absorb (black carbon) or scatter (sulphate aerosols) solar radiation, thus reducing either way the downward flux at the surface [*Smith et al.*, 2011]. This is called the "direct aerosol effect." In addition to scattering and absorption by aerosols particles, a greater number of aerosols may enhance cloud albedo by increasing the number of cloud droplets and consequently the scattering area; known as "indirect aerosols effect" [*Norris and Wild*, 2007].

In this study the analysis of satellite SSR data indicates an overall brightening in the Baltic region from 1984 to 2013, except in winter. Observed SSR changes are at the rate of −0.2, +4.1, +2.8, and +0.3 W/m^2/decade in DJF, MAM, JJA, and SON, respectively (Figure 5). The range of changes of solar radiation solely due to natural climate variability (blue bars in Figure 5), derived from the 1800 year paleosimulations, indicate that the observed trends of SSR in MAM and JJA cannot be explained by natural variations alone ($P < 5\%$). Therefore, we conclude that there are nonnatural drivers at work and that the signal of an anthropogenic forcing is detectable. Climate change projections based on A1B and RCP4.5 scenarios simulate small negative trends in all seasons. As displayed in Figure 5 there is a sign mismatch between observed trends and the response of SSR to GHG forcing simulated by the RCMs. These results provide evidence that the non-GHG anthropogenic signal is detectable. There is, therefore, an additional source of anthropogenic forcing at work, namely, the regionally changing anthropogenic aerosols loadings in the atmosphere.

As shown in Figure 1, none of the RCMs (10 ENSEMBLES; 9 CORDEX) used in this study reproduce the observed warming over the Baltic Sea region in summer and autumn. Over the Euro-Mediterranean region the observed surface solar radiation and land surface temperature spatiotemporal variations are only reproduced when simulations include the realistic aerosols variations [*Nabat et al.*, 2014]. Thus, a possible candidate for explaining the underestimation of warming by RCMs over the Baltic Sea Basin could be the lack

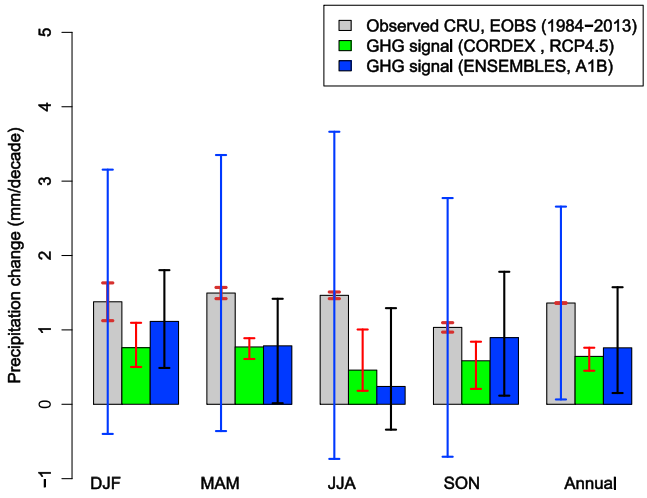

Figure 6. Observed area-averaged precipitation changes over the period 1984–2013 (gray bars) compared to the ensemble mean GHG response estimated from nine CORDEX simulations driven by scenario RCP4.5 (green bars) and 10 ENSEMBLES projections based on SRES A1B (blue bars). The brown whiskers denote the spread in the trends of the two observational data sets (CRU, EOBS). The blue whiskers indicate the 95th percentile uncertainty in the observed trends, derived from the 1800 yearlong paleosimulations. The red and black whiskers show the spread of trends in nine RCP4.5 and 10 A1B climate change projections. Units are mm/decade.

of changing regional aerosol forcing in the models. An alternative explanation is that contemporary regional models do not realistically reproduce the regional response to elevated GHG levels or that the magnitude of natural variability in the paleosimulation underestimates the real natural variability.

6. Precipitation

In terms of precipitation, the study by *Bhend and von Storch* [2008] indicates that the trend pattern of observed precipitation over Northern Europe in winter over the 1973–2002 period match reasonably well the climate change projection. However, the model projections generally underestimate the observed change. Here we show that during the period 1984–2013, both observed data sets (CRU and EOBS) suggest an increase in the amount of precipitation (Figure 6). As shown by blue whiskers in Figure 6, all seasonal precipitation trends in both data sets are not significantly different from natural variability as given by the 1800 year climate simulation of preindustrial conditions. It is interesting to note that, whereas we have not found an equivocal evidence for the presence of nonnatural factors in the observed precipitation trends, the observed trends in winter and autumn lie within the range of changes described by 10 downscaled A1B scenarios. However, when considering the spatial pattern of precipitation change (see Figure S4 in the supporting information), there is an apparent sign mismatch between observed and projected trends over some parts of the region. In summer (JJA) both observation data sets suggest a strong decrease in the amount of precipitation over the southeastern part of the region and over the western part in winter and autumn, which is inconsistent with the increase of precipitation projected by 19 RCMs as response of precipitation to GHG forcing (Figure S4).

The misrepresentation of precipitation trends over Europe depends strongly on the modeled atmospheric circulation and SST trends [*Van Haren et al.*, 2013]. We further examine the possibility that the inconsistency of the climate change projections with the observed precipitation trend patterns may be related to the trends in the large-scale circulation. We compare the observed (NCEP/NCAR reanalysis) [*Kalnay et al.*, 1996] changes in geopotential height at 500 hPa (500 Gph) and in mean sea level pressure with the climate change projections for these two variables (Figures S5 and S6). In summer, a pattern of 500 Gph trends display an area over the southeastern part of the region of increasing geopotential height with +18 m/decade (Figure S5) and also an increase in mean sea level pressure of ~60 Pa/decade (Figure S6). This strengthening of anticyclonic circulation and the decrease in the occurrence of convection due to increasing subsidence thus lead to the drying over the southeastern part of the region, which is inconsistent with the regional future climate projections analyzed here (Figure S4).

7. Conclusions

We have found that the observed warming trend in summer and autumn over the period 1984–2013 is beyond the range attributable to natural variability alone as derived from an 1800 year preindustrial paleosimulations. From this we conclude that the explanation of observed changes in regional temperature require anthropogenic drivers. The results obtained from pattern correlation and regression indicate that the GHG effect markedly contributes to the observed upward trends of temperature. However, in summer

and autumn the observed warming is not consistent with the projected temperature responses to GHG forcing derived from 19 RCMs driven by RCP4.5 and A1B scenarios.

Our analysis also indicates that the effect of an anthropogenic, non-GHG signal, is detectable in surface solar radiation trends during 1984–2013. There is therefore an additional source of anthropogenic forcing. Our findings support that the regionally changing aerosol concentrations may have been responsible for this regional forcing. *Vautard et al*. [2009] indicates that the reduction in low-visibility conditions such as fog, mist, and haze could have contributed to about 50% of eastern European warming. The European sulfur dioxide emissions have decreased since 1980 by about 80%, which has been compensated by increasing emissions elsewhere [*Smith et al*., 2011]. The emissions of aerosol precursors over the Baltic Sea Basin exhibits accelerating increases, with a maximum in the 1970s and a steep decrease in the 1980s (see Figure S3). Since aerosols have mostly a cooling effect, it is plausible that the increased level around the 1980s acted as a brake on the GHG-related warming and that the rapid phasing out of regional aerosol emissions since the 1990s acted as an amplifier of GHG-related warming. At present the aerosol emissions in Europe are at a rather low level, so that future reductions of aerosol emissions will hardly have a noteworthy effect on the regional temperature. Regarding precipitation, the large trends in large-scale circulations over Europe have blurred the externally forced changes, making the detection of anthropogenic climate change very difficult.

Finally, we wish to emphasize that our analysis relies on two significant assumptions. One is that the magnitude of the natural variability as described by the 1800 year paleosimulation is realistic. The second is that climate change signal simulated by the RCMs does not overestimate the true sensitivity of the regional climate system. At this time, we cannot falsify these assumptions, but we need to highlight their presence.

Acknowledgments

We acknowledge the Helmholtz Climate Initiative REKLIM, a joint research project of the Helmholtz Association of German Research Centres (HGF). We further acknowledge the International Detection and Attribution Group (IDAG). We thank anonymous reviewers for valuable comments on the manuscript. A.B. acknowledges the partial support provided by the US National Science Foundation AGS-1547899. J.J.G.N. acknowledges the funding provided through the contract for the return of experienced researches, resolution R-735/2015 of the University of Murcia. Data used in this paper are available from the corresponding author (barkhora@g.ucla.edu) upon request.

References

BALTEX Assessment of Climate Change (BACC) (2015), *Second Assessment of Climate Change for the Baltic Sea Basin*, Springer, Berlin. [Available at http://www.springer.com/gp/book/9783319160054.]

Barkhordarian, A. (2012), Investigating the influence of anthropogenic forcing on observed mean and extreme sea level pressure trends over the Mediterranean region, *Sci. World J.*, *16*, 525303, doi:10.1100/2012/525303.

Barkhordarian, A., H. von Storch, and E. Zorita (2012a), Anthropogenic forcing is a plausible explanation for the observed surface specific humidity trends over the Mediterranean area, *Geophys. Res. Lett.*, *39*, L19706, doi:10.1029/2012GL053026.

Barkhordarian, A., J. Bhend, and H. von Storch (2012b), Consistency of observed near surface temperature trends with climate change projections over the Mediterranean region, *Clim. Dyn.*, *38*, 1695–1702, doi:10.1007/s00382-011-1060-y.

Barkhordarian, A., H. von Storch, and J. Bhend (2013), The expectation of future precipitation change over the Mediterranean region is different from what we observe, *Clim. Dyn.*, *40*, 225–244, doi:10.1007/s00382-012-1497-7.

Bhend, J., and H. von Storch (2008), Consistency of observed winter precipitation trends in northern Europe with regional climate change projections, *Clim. Dyn.*, *31*, 17–28, doi:10.1007/s00382-007-0335-9.

Bhend, J., and H. von Storch (2009), Is greenhouse gas forcing a plausible explanation for the observed warming in the Baltic Sea catchment area?, *Boreal Environ. Res.*, *14*, 81–88, doi:10.1007/s00382-011-1060-y.

Easterling, D. R., and T. C. Peterson (1995), A new method for detecting undocumented discontinuities in climatological time series, *Int. J. Clim.*, *15*, 369–377, doi:10.1002/joc.3370150403.

Flanner, M. G., C. S. Zender, P. G. Hess, N. M. Mahowald, T. H. Painter, V. Ramanathan, and P. J. Rasch (2009), Springtime warming and reduced snow cover from carbonaceous particles, *Atmos. Chem. Phys.*, *9*, 2481–2497, doi:10.5194/acp-9-2481-2009.

Gómez-Navarro, J. J., J. P. Montávez, S. Wagner, and E. Zorita (2013), A regional climate palaeosimulation for Europe in the period 1500–1990—Part 1: Model validation, *Clim. Past*, *9*, 1667–1682, doi:10.5194/cp-9-1667-2013.

Gómez-Navarro, J. J., J. Werner, S. Wagner, J. Luterbacher, and E. Zorita (2015a), Establishing the skill of climate field reconstruction techniques for precipitation with pseudoproxy experiments, *Clim. Dyn.*, *45*, 1395–1413, doi:10.1007/s00382-014-2388-xc.

Gómez-Navarro, J. J., O. Bothe, S. Wagner, E. Zorita, J. P. Werner, J. Luterbacher, C. C. Raible, and J. P. Montávez (2015b), A regional climate palaeosimulation for Europe in the period 1500–1990—Part 2: Shortcomings and strengths of models and reconstructions, *Clim. Past*, *11*, 1077–1095.

Harris, I., P. D. Jones, T. J. Osborn, and D. H. Lister (2014), Updated high-resolution grids of monthly climatic observations—The CRU TS3.10 dataset, *Int. J. Climatol.*, *34*, 623–642, doi:10.1002/joc.3711.

Haylock, M. R., N. Hofstra, A. M. G. Klein Tank, E. J. Klok, P. D. Jones, and M. New (2008), A European daily high-resolution gridded dataset of surface temperature and precipitation, *J. Geophys. Res.*, *113*, D20119, doi:10.1029/2008JD10201.

Hegerl, G., J. Luterbacher, F. Gonzalez-Rouco, S. F. B. Tett, T. Crowley, and E. Xoplaki (2011), Influence of human and natural forcing on European seasonal temperatures, *Nat. Geosci.*, *4*, 99–103.

Intergovernmental Panel on Climate Change (2013), *Climate Change 2013: The Physical Science Basis. Contribution of Working Group I to the Fifth Assessment Report of the Intergovernmental Panel on Climate Change*, 1535 pp., Cambridge Univ. Press, Cambridge, U. K., and New York.

Jacob, D., et al. (2014), EURO-CORDEX: New high resolution climate change projections for European impact research, *Reg. Environ. Change*, *14*, 563–578.

Jones, C., F. Giorgi, and G. Asrar (2011), The Coordinated Regional Downscaling Experiment: CORDEX; An international downscaling link to CMIP5, CLIVAR Exchanges, No. 56, pp. 34–40, International CLIVAR Project Office, Southampton, U. K.

Jones, P. W. (1999), First- and second-order conservative remapping schemes for grids in spherical coordinates, *Mon. Weather Rev.*, *127*, 2204–2210.

Kalnay, E., et al. (1996), The NCEP/NCAR 40-year reanalysis project, *Bull. Am. Meteorol. Soc.*, *77*, 437–471.

Kjellström, E., P. Thejll, M. Rummukainen, J. H. Christensen, F. Boberg, O. B. Christensen, and C. Fox Maule (2013), Emerging regional climate change signals for Europe under varying large-scale circulation conditions, *Clim. Res.*, *56*, 103–119, doi:10.3354/cr01146.

Legutke, S., and E. Maier-Reimer (1999), Climatology of the HOPE-G global ocean general circulation model, *Tech. Rep.*, *21*, 90 pp., German Climate Computer Centre (DKRZ), Hamburg, Germany.

Meinshausen, M., et al. (2011), The RCP greenhouse gas concentrations and their extension from 1765 to 2300, *Clim. Change.*, doi:10.1007/s10584-011-0156-z.

Nabat, P., S. Somot, M. Mallet, A. Sanchez-Lorenzo, and M. Wild (2014), Contribution of anthropogenic sulfate aerosols to the changing Euro-Mediterranean climate since 1980, *Geophys. Res. Lett.*, *41*, 5605–5611, doi:10.1002/2014GL060798.

Nakicenovic, N., et al. (2000), *Special Report on Emissions Scenarios: A Special Report of Working Group III of the Intergovernmental Panel on Climate Change*, 599 pp., Cambridge Univ. Press, Cambridge, U. K.

Norris, J. R., and M. Wild (2007), Trends in aerosol radiative effects over Europe inferred from observed cloud cover, solar "dimming" and solar "brightening", *J. Geophys. Res.*, *112*, D08214, doi:10.1029/2006JD007794.

Peings, Y., and G. Magnusdottir (2014), Forcing of the wintertime atmospheric circulation by the multidecadal fluctuations of the North Atlantic Ocean, *Environ. Res. Lett.*, *9*, 034018, doi:10.1088/1748-9326/9/3/034018.

Posselt, R., R. Mueller, R. Stockli, and J. Trentmann (2011), Spatial and temporal homogeneity of solar surface irradiance across satellite generations, *Remote Sens.*, *3*, 1029–1046, doi:10.3390/rs3051029.

Roeckner, E., et al. (1996), The atmospheric general circulation model ECHAM-4: Model description and simulation of present-day climate, *Rep. 218*, 90 pp., Max Planck Inst. for Meteorol., Hamburg, Germany.

Smith, S. J., J. van Aardenne, Z. Klimont, R. J. Andres, A. Volke, and S. Delgado Arias (2011), Anthropogenic sulfur dioxide emissions: 1850–2005, *Atmos. Chem. Phys.*, *11*, 1101–1116, doi:10.5194/acp-11-1101-2011.

Stott, P. A., et al. (2010), Detection and attribution of climate change: A regional perspective, *WIREs: Clim. Change*, *1*, 192–211, doi:10.1002/wcc.34.

Van Haren, R., G. J. van Oldenborgh, G. Lenderink, M. Collins, and W. Hazeleger (2013), SST and circulation trend biases cause an underestimation of European precipitation trends, *Clim. Dyn.*, *40*, 1–20, doi:10.1007/s00382-012-1401-5.

van Oldenborgh, G. J., S. Drijfhout, A. van Ulden, R. Haarsma, A. Sterl, C. Severijns, W. Hazeleger, and H. Dijkstra (2009), Western Europe is warming much faster than expected, *Clim. Past*, *5*, 1–12, doi:10.5194/cp-5-1-2009.

Vautard, R., P. Yiou, and G. J. van Oldenborgh (2009), Decline of fog, mist and haze in Europe over the past 30 years, *Nat. Geosci.*, *2*, 115–119, doi:10.1038/NGEO414.

Wild, M., H. Gilgen, A. Roesch, A. Ohmura, C. N. Long, E. G. Dutton, B. Forgan, A. Kallis, V. Russak, and A. Tsvetkov (2005), From dimming to brightening: Decadal changes in solar radiation at Earth's surface, *Science*, *308*, 847–850, doi:10.1126/science.1103215.